Astron. Astrophys. 344, 632–638 (1999)

ASTRONOMY
AND
ASTROPHYSICS

The origin of the protostellar jet GGD 34⋆

Ana I. Gómez de Castro[1] **and Angel Robles**[1]

Instituto de Astronomía y Geodesia (CSIC-UCM), Facultad de CC. Matemáticas, Universidad Complutense de Madrid (UCM), E-28040 Madrid, Spain (aig@eucmos.sim.ucm.es; angel@orion.mat.ucm.es)

Received 7 July 1998 / Accepted 18 January 1999

Abstract. GGD 34 is a protostellar jet with wiggles which are accompanied by "sine-like" variations in the radial velocity of the emitting material by as much as 60 km s^{-1}. Thus GGD 34 is an interesting object to understand the physical mechanisms involved in the generation of wiggles in protostellar jets.

In this work we present high resolution images obtained with the Canada-France-Hawaii Telescope (CFHT) which shows that GGD 34 consists of a narrow (unresolved) jet roughly bisecting an extended faint envelope. The [S II] emission from the working surface has an arrow shaped morphology; the body of the jet is clearly distinguished as well as two backtails disposed in an approximately symmetric manner with respect to the jet axis. The Hα emission is concentrated at the head of the jet indicating that the gas is significantly more excited at this location (in particular at the so-called Knot 5); we suggest that Knot 5 traces the location of the Mach disk since spectra of GGD 34 indicate that it is a light beam of gas. The high resolution images also show that the envelope around GGD 34 connects smoothly with the back tails at the head of the jet. We speculate whether it traces the backflow; the expected backflow velocity is shown to be ~ 32 km s^{-1} which is consistent with the degree of excitation of the envelope. However, an accurate determination of the proper motion of the head is necessary to check whether this interpretation is correct.

We also present radiocontinuum (3.6 and 6 cm) VLA observations and report the detection of a radio source close to the apex of the cavity from which the jet emerges. This radio source has a spectral index of 0.7 ± 0.5, consistent within error with the value of 0.6 expected for a thermal jet. We suggest that this radio object is associated with the source of the outflow. Additional ^{12}CO(3–2) observations obtained with the JCMT show molecular gas redshifted by ~ 2.5 km s^{-1} with respect to the cloud at this location.

Key words: stars: mass-loss – stars: pre-main sequence – ISM: individual objects: GCD 34 – ISM: jets and outflows – radio continuum: ISM – radio lines: ISM

Send offprint requests to: Ana I. Gómez de Castro

⋆ Based on observations carried out at the Calar Alto, CFHT, VLA and JCMT

1. Introduction

Optical jets from young stellar objects (YSOs) often display wiggles or small departures from strict cylindrical symmetry when looked at with high enough spatial resolution (see e.g. HH 46/47 (Heathcote et al. 1996)). These distortions have been accounted for two main physical mechanisms namely, variations in the direction of the outflow axis (Raga et al. 1993; Biro et al. 1995) or jet instabilities (Camenzind 1997; Stone 1997; Massaglia et al. 1997). Both mechanisms may be acting in one way or another in YSOs jets.

GGD 34 is a unique protostellar jet for this type of study because its morphology and radial velocity field seem to be well correlated as shown by Gómez de Castro et al. (1993). GGD 34 is located in NGC 7129, a well known star forming region at 1 kpc from the Sun (Racine 1968). The object consist of three major condensations aligned over 0.17 pc which are embedded in a weak envelope emitting primarily in [S II] (Hartigan & Lada 1985; Strom et al. 1986; Ray 1987; Gómez de Castro 1989; Eiroa et al. 1992; Gómez de Castro et al. 1993). The westernmost condensation has a significant reflection component that most likely traces the bow-shaped borders of the cavity illuminated by the exciting star. The source of the flow has not yet been identified. Spectra of GGD 34 have been published by Goodrich (1986), Movsessian (1992) and Gómez de Castro et al. (1993). The spectra show emission lines of low ionization or neutral species such as [O I] or [S II]; the post-shock electron density is very low: $< 10^2$ cm^{-3} (Goodrich 1986; Movsessian 1992; Gómez de Castro et al. 1993). The radial velocity field along the jet can be well fitted to a sine curve with mean velocity ~ -180 km s^{-1} and maximum of -240 km s^{-1} (Gómez de Castro et al. 1993). Recent independent studies confirm this behaviour (Magakian & Movsesian 1997). The correlation between the morphology and the radial velocity field, as well as the lack of a correlation between the velocity field and the excitation conditions of the gas, led Gómez de Castro et al. (1993) to suggest that the variations are associated with geometric distortions that could be induced by the onset of an instability in the jet.

In this work we present high resolution images of GGD 34 obtained with the CFHT and the High Resolution Camera (HRCam). The comparison between these new images with

previous lower spatial resolution images (Ray 1987; Eiroa et al. 1992; Gómez de Castro et al. 1993) suggests that the large scale wiggles are most likely associated with a low-surface-luminosity nebula emitting primarily in [S II]; the jet itself being well collimated. Nevertheless, we emphasize that the jet does wiggle from side to side although the amplitudes of its oscillations are much smaller than in the case of the nebula. Note also that the huge amount of energy needed to feed distortions in the jet of 10% of its length makes them very improbable anyway and that such distortions have never been seen before in much more closer jets (e.g. the distance to NGC 7129 is 7 times the distance to Taurus i.e. 140 pc (Elias 1978)).

We also present radiocontinuum (3.6 and 6 cm) VLA observations intended to search for the source of the outflow. ^{12}CO(3–2) line observations have also been obtained to study the perturbations produced by the jet in the heavily stirred environment of the NGC 7129 molecular cloud. The observations are described in Sect. 2. The VLA data are used in Sect. 3 to identify the source of jet. In Sect. 4 we study the structure of GGD 34 in view of the new optical images. The variability of the jet is analyzed in Sect. 5. A brief discussion on the nature of the envelope is given in Sect. 6 and the main conclusions of the work are summarized in Sect. 7.

2. Observations

2.1. Optical images

Optical images were obtained in October 1991 with the High Resolution Camera (HR Cam) of the CFHT. This camera enabled us to obtain images with spatial resolution of 0.5–0.8 arcsec (500–800 AU at NGC 7129). We employed the SAIC 1 CCD which has a field of view of 2.2 x 2.2 arcmin and a pixel size of 18 μm. The scale is 0.13 arcsec/pixel (see McClure et al. 1989 for details on HR Cam).

We obtained images in two narrow band filters with the specifications; Hα ($\lambda_c = 6567$ Å and FWHM = 30 Å) and [S II] ($\lambda_c = 6729$ Å and FWHM = 47 Å; both 6716 Å and 6731 Å lines are transmitted). We also used a broad band I filter. We obtained four images in each bandpass for a total exposure time of 1 hour in the narrow band filters and a total of 15 minutes for the I band image. The data were reduced using the Munich Image Data Analysis System. Images are bias-corrected and flat-fielded in the standard manner. Images with similar good seeing have been co-added to obtain the images shown in Fig. 1.

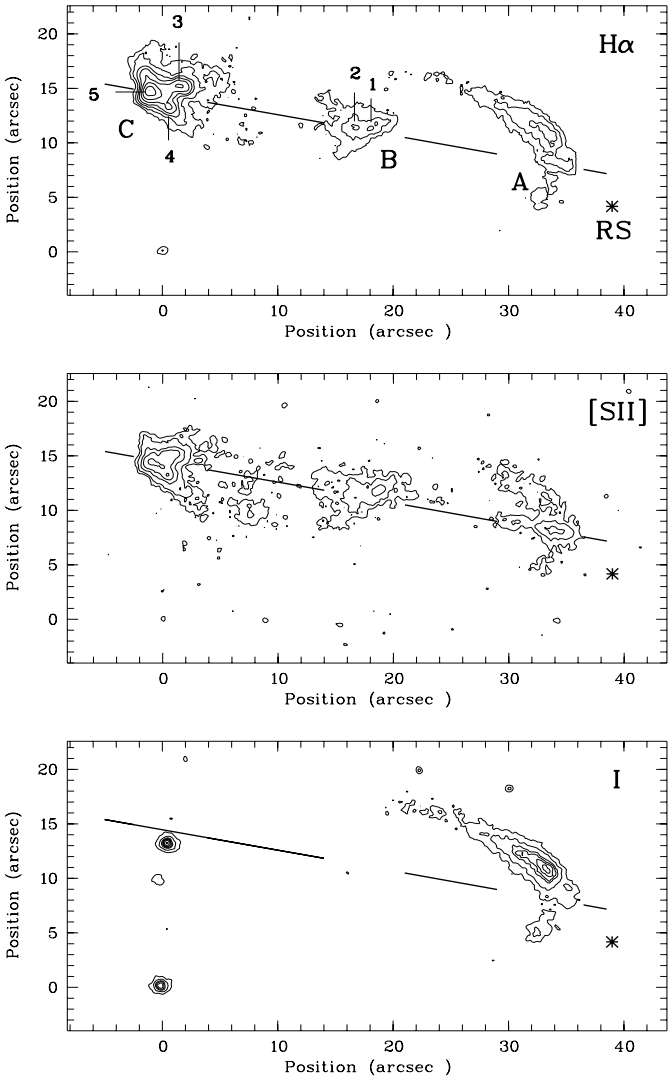

Fig. 1. Optical images of GGD 34. The condensations are named following Gómez de Castro et al. (1993) in order of increasing right ascension. The orientation corresponding to position angle +79° is shown by a straight line. The 5 main knots are marked on top of the Hα image. The position of the radio source is also marked with an asterisk.

2.2. 3.6 cm and 6 cm radiocontinuum observations

The GGD 34 region was observed at 3.6 and 6 cm using the Very Large Array of NRAO. The dates and other parameters of the observations are given in Table 1. The observations were made in the continuum mode with an effective bandwidth of 100 MHz. The data were calibrated and natural weight maps were made using the tasks of the Astronomical Image Processing System. The 3.6 cm data was tapered slightly to produce 3.6 and 6 cm maps of comparable angular resolution (about 5 arcsec). The maps are shown in Fig. 2. A faint, unresolved radio source was detected south west of GGD 34. The parameters of this source are given in Table 2.

2.3. ^{12}CO(3–2) observations

A low resolution mosaic of ^{12}CO(3–2) emission (excited molecular gas) around GGD 34 was kindly provided by R. Padman. The ^{12}CO(3–2) observations were made with the James Clerk Maxwell Telescope (JCMT) in January 1993. The map is centred at α(1950)=21$^{\rm h}$42$^{\rm m}$18$^{\rm s}$.28, δ(1950)=65°55′00″ coinciding approximately with the position of the central condensation: GGD 34/B. The spatial resolution of the map is of 14″. The grid of observed positions consists of an ensemble of 5 parallel east-west strips sampled every 7″. The sampling in the north-south direction was the same but 7 strips were made in total.

Table 1. GGD 34 VLA observations

Epoch	VLA Configuration	Wavelength (cm)	Phase Calibrator	Bootstrapped Flux Density (Jy)	Synthesized Beam	rms noise (μJy)
1990 Nov 24	C	3.6	2146+608	0.892±0.003	$5\farcs2\times4\farcs8$; 0°	21
1992 Feb 20	B/C	6	2146+608	1.067±0.006	$6\farcs6\times4\farcs5$; 0°	27

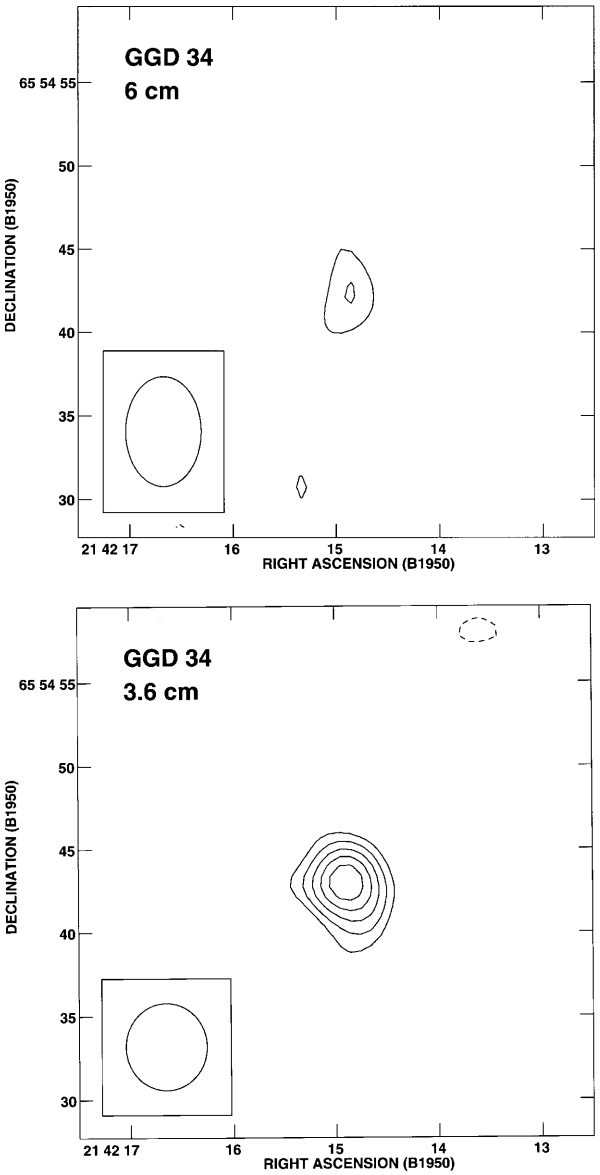

Fig. 2. VLA maps at 6 cm (*top panel*) and 3.6 cm (*bottom panel*) of the GGD 34 region. The synthesized beam is shown in the bottom left corner of each panel. The contours are -3, 3, 4, 5, 6, and 7 times the rms noise of the maps (27 μJy for 6 cm and 21 μJy for 3.6 cm).

3. The exciting source

The radio source is located to the southwest of GGD 34 and appear projected at the edge of the ammonia condensation mapped by Torrelles et al. (1983). It has a spectral index of 0.7± 0.5.

Table 2. Parameters of detected VLA source

α^{a}(1950)	δ^{a}(1950)	$S_{6\,cm}$(mJy)	$S_{3.6\,cm}$(mJy)	Spectral Index
$21^{h}42^{m}14\fs90$	$+65°54'43\farcs0$	0.12 ± 0.03	0.17 ± 0.02	0.7 ± 0.5

[a] Positional accuracy is $\sim 0\farcs5$

Within the error, this spectral index is consistent with the value of 0.6 expected for a thermal jet (Rodríguez 1997). The confirmation of this source as a thermal jet would require a high angular resolution map to search for the elongated morphology, aligned with the outflow axis, that characterizes these sources. Unfortunately, the source is too faint for this. The radio source is most probably associated with the optical jet on two grounds. First, most background sources have negative spectral indices, while the source detected has a positive spectral index. Second, the *a priori* possibility of having a background 3.6 cm source with a flux density of 0.17 mJy inside a solid angle of 0.2 square arcmin is only ∼0.01. The ^{12}CO(3–2) observations also show some degree of activity in this area (the south-west border) of the map in that gas, redshifted by ~ 2.5 km s^{-1} with respect to the cloud emission, is detected at this location. This redshifted gas suggestively lies opposite the optical blueshifted jet and seems to be associated with the VLA source so it could be tracing the receeding part of the flow. Unfortunately the spatial resolution, and especially the coverage of our map, is not good enough to determine whether it is associated with the VLA source or with a nearby structure. Note that NGC 7129 is a very active region of star formation.

The location and properties of the radio source suggest that it may be embedded in a cloud core and excite GGD 34 to its east, outside this core, producing an optically visible object. The radio source is nearly aligned with the jet axis: it is $2\farcs9$ south of the axis and only $3''$ westwards of the cavity (GGD 34/A). Recent, H_2 and K-band images of NGC 7129 show the presence of an extended nebulosity in this area which is most likely caused by scattered light from the exciting source of GGD 34 (Palacios et al. 1997). The nebulosity extends southwest from the optical cavity in the direction of the VLA source. No IRAS counterpart to the VLA source has been found in the point sources catalogue. At a distance of 1 kpc, the VLA source has a radio "luminosity" of about 0.17 mJy kpc^2. This luminosity is typical of low bolometric luminosity YSOs as discussed by Anglada (1996). If the source were at the distance of Orion, its flux density would be comparable with that of HH 1-2 VLA1, the source that excites this classic Herbig-Haro system (Rodríguez 1990).

Table 3. Characteristics of the main knots in GGD 34

Knot	α(1950)	δ(1950)	FWHM(Hα)	FWHM([S II])	I(Hα)/I([S II])[a]
1	$21^{\rm h}42^{\rm m}18\overset{\rm s}{.}10$	$65°54'49\overset{''}{.}8$			1.00
2	$21^{\rm h}42^{\rm m}18\overset{\rm s}{.}46$	$65°54'48\overset{''}{.}9$			1.13
3	$21^{\rm h}42^{\rm m}21\overset{\rm s}{.}00$	$65°54'53\overset{''}{.}0$	$1\overset{''}{.}22$		1.79
4	$21^{\rm h}42^{\rm m}21\overset{\rm s}{.}14$	$65°54'51\overset{''}{.}3$	$0\overset{''}{.}93$	$0\overset{''}{.}25$	1.26
5	$21^{\rm h}42^{\rm m}21\overset{\rm s}{.}37$	$65°54'52\overset{''}{.}4$	$1\overset{''}{.}48$	$1\overset{''}{.}50$	2.11

[a] The intensity ratios are normalized to the ratio in Knot 1.

4. The structure of the jet

4.1. The base

The new VLA observations indicate that the source driving GGD 34 is deeply embedded. The source illuminates a reflection nebula that surrounds the base of the jet and extends along the northeastern edge. There is a clear brightness minimum in the I-band image at the apex of the nebula through which the optical jet emerges (see Fig. 1); the jet has excavated its way through the nebula outwards from the cloud core. The nebula is brighter in Hα than in [S II] because the star has strong Hα emission (Gómez de Castro et al. 1993), this produces a noticeable apparent "misalignment" between the jet orientation in the Hα and [S II] images. The [S II] emission is well aligned with the major axis of GGD 34, however the Hα emission is $\sim 17°$ NE of the major axis. This "misalignment" readily disappears when the nebular contribution is subtracted out.

4.2. The body

The body of the jet is seen primarily in [S II]. The improved resolution CFHT images show a narrow jet which roughly bisects an extended faint envelope. The peak emission of condensations B and C is well aligned with the major axis however the condensations themselves are markedly non-axisymmetric. The jet shows wiggling and several abrupt changes in its apparent direction in GGD 34/B.

The width of the jet is unresolved. There are 5 main knots, shown in the Hα panel of Fig. 1, whose coordinates are given in Table 3 in order of increasing right ascension. Two of them are associated with GGD 34/B and 3 with GGD 34/C. The size of some knots within GGD 34/C is resolved. These sizes are given in Table 3 assuming a gaussian transfer function for the optical system with FWHM=$0\overset{''}{.}7$; they are typically between 0.3 and 1.5 arcsec (300–1500 AU). These sizes are significantly larger than the inferred from recent HST images of YSOs jets ($\sim$ 100 AU size) suggesting that they may be constituted of finer structures unresolved in the CFHT images.

The ratio of Hα to [S II] fluxes is often used as a diagnostic of shock strength with larger ratios corresponding to higher shock velocities for shock velocities smaller than 80 km s^{-1} (Hartigan et al. 1987). The Hα/[S II] ratio for the knots in GGD 34 is also given in Table 3. These values are normalized to the Hα/[S II] ratio in Knot 1. The excitation is significantly larger in the Knots 3 and 5 than in the rest of the jet suggesting larger shock velocities at these points. In particular, the Hα/[S II] ratio is a factor of 2 larger in Knot 5 than in Knots 1, 2 or 4.

4.3. The working surface

The optical jet ends at GGD 34/C. The [S II] emission region has an arrow or bow-shaped morphology; the body of the jet is clearly distinguished as well as two back tails disposed in an approximately symmetric manner with respect to the jet axis. The Hα emission is concentrated at the head of the jet (Knot 5); the two back tails also emit in the Hα line but the northern (Knot 3) is significantly brighter than the southern (Knot 4) while in [S II] both have similar strengths. There is a protrusion NE off the axis which emits mainly in Hα. These characteristics are better summarized in Fig. 5, where the Hα $-$[S II] image of the head of the jet is represented. The Hα emission dominates at the head of the jet (Knot 5), in the protrusion and in Knot 3. This high degree of excitation as well as its morphology (note the flat head of Knot 5) suggest that GGD 34/C marks the location of the working surface of the jet. In the simplest case the working surface consists of a bow shock where the ambient material is accelerated and a jet shock or Mach disk, where the jet material is decelerated. The Mach disk is the stronger shock when the jet is less dense than the ambient medium, while the bow shock is stronger for heavy jets.

The spectra of GGD 34 indicate that it is a beam of relatively light gas with respect to its ambient environment; the ratio between the intensities of the [S II] lines, I6717/I6730 is $\sim 1.3 - 1.4$ (Goodrich 1986; Gómez de Castro et al. 1993) implying post-shock electron densities of 30 to 60 cm^{-3}. The low excitation degree of the gas suggests small ionization fractions $\chi \sim 10\%$ which points to post-shock jet particle densities of $\rm N_j \sim 300$–$600\,cm^{-3}$. These values are smaller than the average density of the molecular cloud in this area which is $\sim 10^3$ cm^{-3} (Bechis et al. 1978). Note moreover, that there is a very steep luminosity gradient at the eastern edge of GGD 34/C (Knot 5) suggesting that the outflow has encounter an obstacle denser than the cloud environment. This makes us suspect that the brighter shock in GGD 34/C is the jet shock and that therefore Knot 5 is tracing the Mach disk. The fact that it emits strongly in Hα is also consistent with the jet being mostly neutral. Existing spectra have not enough spatial resolution to resolve its kinematical signatures (Goodrich 1986; Gómez de Castro et al. 1993; Magakian & Movsesian 1997). It is tempting to associate the sudden decrease in radial velocity in GGD 34/C with the Mach disk.

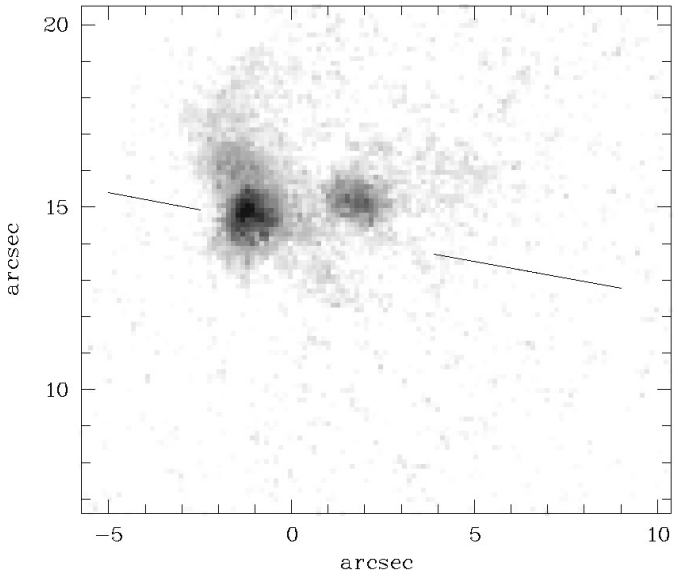

Fig. 3. Hα-[S II] image of the working surface (GGD 34/C). The scale has been selected so dark grey corresponds to the maximum Hα emission and white to the maximum [S II] emission. The scale enhances the most relevant features. North is up and East to the left.

However, this deceleration is more evident at the north-east end, and it is best traced in Hα than in [S II] indicating that it is most likely associated with the protrusion. This protrusion is probably tracing the path of the flow after a grazing collision with some obstacle; maybe some material could also be entrained by the jet at this point.

5. Optical variability

The CFHT images have been compared in detail with those obtained in July 1988 with the 3.5 m telescope of the Calar Alto Observatory. The Calar Alto images have a scale of $0\farcs254$ pix^{-1} and were obtained with an RCA CCD with 15 μm pixel size. The filters used were: broad-band I ($\lambda_{\rm eff} = 9140$ Å and $\Delta\lambda = 2000$ Å at the 10% level), Hα ($\lambda_{\rm eff} = 6567$ Å and FWHM = 100 Å) and [S II] ($\lambda_{\rm eff} = 6730$ Å and FWHM = 95 Å). The seeing was $\sim 1''$. A more detailed description of the images and their reduction is given in Gómez de Castro et al. (1993).

We have not found significant changes in GGD 34 between the two epochs when viewed through the I filter; both morphology and relative intensities remain rather constant. There are however variations between the two [S II] and the two Hα frames. The intensity of GGD 34/C relative to this of GGD 34/A has decreased by a factor of 0.25 from 1988 to 1991 in the Hα and [S II] images.

No proper motions are detected after comparison of the 1991 images with those obtained in 1988; this is consistent with previous determinations (Ray et al. 1990).

6. On the nature of the GGD 34 envelope

The most puzzling characteristic of GGD 34 is the presence of the extended faint envelope forming a bubble like shell between GGD 34 B and C. The envelope emits more strongly in [S II] than in Hα and it is better observed in images with low spatial resolution (see e.g. Ray 1987). The new CFHT images show that the envelope connects smoothly with the back tails at the head of the jet suggesting that it can be tracing, at least partially, the backflow.

Strong backflows are expected particularly in low density, high Mach number jets. The jet material, which is still travelling forwards after passing through the jet-shock, is bent back towards the source by the pressure gradient between the shocked molecular cloud at the head of the jet (i.e. material at the stand-off shock in the jet) and the thermal pressure of the material jet. The strength of the backflow depends both on the density ratio and the Mach number of the jet, however for sufficiently light jets the shock front can be considered as stationary and therefore the dependence of the backflow strength on density ratio is very weak. Williams (1991) has computed the expected relationship between the Mach number of the backflow ($\rm M_b$) and the jet Mach number ($\rm M_j$) *in the case of no turbulence and a tangled magnetic field*, which for the adiabatic case (i.e. we are neglecting radiative cooling at the head of the jet) with adiabatic index γ = 5/3 is:

$$\rm M_b^2 = 3 \times [1.1662 \times M_j^{2/5} - 1]$$

The Mach number of GGD 34 is very high. The velocity of the jet, $\rm V_j$ is:

$$\rm V_j = \sqrt{V_r^2 + V_{pm}^2} = \sqrt{(-180)^2 + (110)^2} = 211\ km\ s^{-1}$$

where $\rm V_r$ is the mean radial velocity which is -180 km s^{-1} according to Gómez de Castro et al. (1993) and $\rm V_{pm}$ is the velocity in the plane of the sky determined by Ray et al. (1990) from the proper motion of the head of the jet. Note that $\rm V_j$ determined in this way represents a lower limit to the true jet speed since given the variability and the complex structure of the head an accurate determination of the proper motion requires the comparison between high resolution images. The jet sound speed is ~ 11 km s^{-1} assuming a fiducial temperature of 10^4 K. Therefore, the Mach number of GGD 34 is:

$$\rm M_j = \frac{V_j}{c_s} = 19.2 \times (\frac{T}{10^4 K})^{1/2}$$

As a consequence the expected Mach number of the backflow is,

$$\rm M_b^2 = 3 \times [20.4 \times (\frac{T}{10^4 K})^{1/5} - 1]$$

This implies a backflow speed of $\sim$ 32 km s^{-1}. This flow is clearly supersonic in the molecular environment; the sound speed inferred from the CO lines excitation temperatures in this area of NGC 7129 is 0.4 km s^{-1} (Bechis et al. 1978). Shocks at this velocity are expected to emit primarily in [S II] (see Heathcote et al. 1996 for a detailed discussion on the structure of the shocks at these low velocities) and this could explain why, in general, the envelope is brighter in [S II] than in Hα. No indications of such a low velocity gas have been found in the optical

spectra but this could be due to the low surface brightness of the envelope which would require much longer integration times in order to detect its spectroscopic signature.

Additional constraints to this interpretation can be derived from a comparison between the dynamical time-scale for the formation of the envelope and the dynamical time-scale for the formation of the jet; the envelope extends roughly over a half of the jet length and the velocity of the backflow is a factor of 0.15 the jet speed. The dynamical time for the formation of GGD 34 is:

$$\tau_{\rm GGD\ 34} = \frac{\rm L_{GGD\ 34}}{\rm V_j}$$

where $\rm L_{GGD\ 34}$ represents the length of the jet. The proper motion measured by Ray et al. (1990) indicates that GGD 34 is highly inclined with respect to the plane of the sky. We derive an inclination of:

$$i = \arctan(\frac{\rm V_r}{\rm V_{pm}}) = 58\overset{\circ}{.}6$$

and a length of the jet of:

$$\rm L_{GGD\ 34} = 0.19pc \times (\cos\, \it i)^{-1} = 0.37pc$$

This implies a dynamical time of $\tau_{\rm GGD\ 34} = 1.7 \times 10^3$ yrs. However the time required by the backflow to form the envelope is:

$$\tau_{\rm env} = \frac{\rm L_{env}}{\rm V_b} = 5 \times 10^3 \ {\rm yrs}$$

where $\rm L_{env}$ represents the length of the envelope (0.16 pc) and $\rm V_b$ the backflow speed. This time is a factor of 2 larger than the jet dynamical time scale which, in principle, is inconsistent with the envelope being produced by the jet backflow. Note however, that the dynamical time scale of the flow is just a lower limit to the jet true age. If the jet is light and the head has remained stationary during most of the jet life, the age of the jet could be significantly larger than the $\tau_{\rm GGD\ 34}$ calculated above. A good estimate of the proper motion of the head based on high resolution images is clearly required.

7. Summary and conclusions

We have presented in this work a set of observations intended to search for the exciting source of the jet GGD 34 and study the detailed structure of the outflow. Our main results are:

- We have found a radio source close to the apex of the cavity from which the jet emerges. This radio source has a spectral index of 0.7±0.5, consistent with the value of 0.6 expected for a thermal jet. The ^{12}CO(3–2) observations show molecular gas redshifted by $\sim$ 2.5 km s^{-1} with respect to the cloud at this location.
- The improved resolution of the CFHT images show that GGD 34 is a narrow (unresolved) jet which roughly bisects an extended faint envelope. The jet is visible at three points along its length: at the base where it emerges from the cloud core (GGD 34/A), at the head where the working surface is (GGD 34/C) and at approximately the middle point (GGD 34/B).
- We have identified 5 main knots in the jet. Some of them are resolved; they are typically between 0.9 and 1.5 arcsec (900–1500 AU) in size. These sizes are significantly larger than the inferred from recent HST images of YSOs jets suggesting that they may be composed of finer structures unresolved in the CFHT images. The Hα/[S II] ratio has been determined for the knots indicating that the gas is significantly more excited at the head of the jet and, particularly, in Knot 5.
- The high resolution images show that the [S II] emission from the working surface has an arrow shaped morphology; the body of the jet is clearly distinguished as well as two backtails disposed in an approximately symmetric manner with respect to the jet axis. The Hα emission is concentrated at the head of the jet. We suggest that Knot 5 traces the location of the Mach disk since the spectra of GGD 34 suggest that its density is low with respect to its external environment.
- We have compared images obtained several years apart and we have not obtained any measurable proper motions. We have however detected changes in the excitation degree of the head of the jet.
- The high resolution images show that the envelope around GGD 34 connects smoothly with the back tails at the head of the jet. We have examined whether this envelope could be tracing backflow from the jet and show that although the expected velocity of this backflow (32 km s^{-1}) is consistent with the degree of excitation of the envelope, the time required to form the observed envelope is twice the dynamical time scale of the jet.

In summary, the new images have shown that the GGD 34 jet is a narrow (unresolved) beam of gas with small wiggles which are alike those observed in other YSO jets. However the origin of the asymmetric low-surface luminosity envelope which surrounds the jet remains uncertain as well as the cause of the peculiar radial velocity field along the jet. High spatial resolution long slit spectroscopy is required to separate the contribution of the envelope to the GGD 34 spectrum and get further insight into this object characteristics. Good measurements of GGD 34's proper motions are also necessary.

Acknowledgements. We are indebted to Rachael Padman for providing us with the ^{12}CO(3–2) map of the GGD 34 area and to Luis F. Rodríguez for the VLA data. We thank Stefan Appl, Pierre Bastien, Philip Hardee and Ralph E. Pudritz for stimulating conversations on jets physics. We also thank the staff at the CFHT and at the VLA for their support during the observations and very especially Robert McClure for his very helpful comments on CFHT+HRCam optical properties. We are grateful to the referee for his/her thorough revision of the english. This work was partially supported by the Spanish Ministerio de Educación y Ciencia (MEC) through grant PB93-0491 and the Universidad Complutense de Madrid (UCM) through grant PR156/97-7136.

References

Anglada G., 1996, In: Taylor A.R., Paredes J.M. (eds.) Radio Emission from the Stars and the Sun. ASP, San Francisco, 3
Bechis K.P., Harvey P.M., Campbell M.F., Hoffmann W.F., 1978, ApJ 226, 439
Biro S., Raga A.C., Cantó J., 1995, MNRAS 275, 557
Camenzind M., 1997, In: Reipurth B., Bertout C. (eds.) Herbig-Haro Flows and the Birth of Low Mass Stars. Proceedings of IAU Symp. No. 182, Kluwer, Dordrecht, p. 241
Eiroa C., Gómez de Castro A.I., Miranda L.F., 1992, A&AS 92, 721
Elias J.H., 1978, ApJ 224, 859
Gómez de Castro A.I., 1989, Ph.D. Thesis, Universidad Complutense de Madrid
Gómez de Castro A.I., Miranda L.F., Eiroa C., 1993, A&A 267, 559
Goodrich R.W., 1986, AJ 92, 885
Hartigan P., Lada C.J., 1985, ApJS 59, 383
Hartigan P., Raymond J.,Hartmann L., 1987, ApJ 316, 323
Heathcote S., Morse J.A., Hartigan P., et al., 1996, AJ 112, 1141
Magakian T.Y., Movsesian T.A., 1997, A.Rep. 41, 483
Massaglia S., Micono M., Ferrari A., Bodo G., Rossi P., 1997, In: p. 335
McClure R.D., Grundmann W.A., Rambold W.N., et al., 1989, PASP 101, 1156
Movsessian T.H., 1992, Pis'ma Astron. Zh. 18, 748
Palacios J., Eiroa C., Miranda L.F., 1997, In: Malbet F., Castets A. (eds.) Low Mass Star Formation – from Infall to Outflow. Poster proceedings of IAU Symp. No. 182, p. 30
Racine R., 1968, AJ 73, 233
Raga A.C., Cantó J., Biro S., 1993, MNRAS 260, 163
Ray T.P., 1987, A&A 171, 145
Ray T.P., Poetzel R., Solf J., Mundt R., 1990, ApJ 357, L45
Rodríguez L.F., Curiel S., Ho P.T.P., et al., 1990, ApJ 352, 645
Rodríguez L.F., 1997, in Herbig-Haro Flows and the Birth of Low Mass Stars, proceedings of IAU Symp. No. 182, eds. B. Reipurth & C. Bertout, (Dordrecht: Kluwer) p. 83
Stone J.M., 1997, In: Reipurth B., Bertout C. (eds.) Herbig-Haro Flows and the Birth of Low Mass Stars. Proceedings of IAU Symp. No. 182, Kluwer, Dordrecht, p. 323
Strom K.M., Strom S.E., Wolff S.C., Morgan J., Wenz M., 1986, ApJS 62, 39
Torrelles J.M., Rodríguez L.F., Cantó J., et al., 1983, ApJ 274, 214
Williams A.G., 1991, In: Hughes P.A. (ed.) Beams and Jets in Astrophysics. Cambridge University Press, p. 342